Biochemical and Biophysical Research Communications 414 (2011) 209–214

Contents lists available at SciVerse ScienceDirect

Biochemical and Biophysical Research Communications

journal homepage: www.elsevier.com/locate/ybbrc

Molecular ruler of tripeptidylpeptidase II: Mechanistic principle of exopeptidase selectivity

Jürgen Peters *, Anne-Marie Schönegge, Beate Rockel, Wolfgang Baumeister

Max-Planck-Institute of Biochemistry, Department of Molecular Structural Biology, Am Klopferspitz 18, 82152 Martinsried, Germany

ARTICLE INFO

Article history:
Received 7 September 2011
Available online 16 September 2011

Keywords:
Tripeptidylpeptidase II
Double-Glu motif
Molecular ruler
Aminotripeptidase
Kinetic study

ABSTRACT

The structure of tripeptidylpeptidase II (TPPII) has shown that it belongs to the group of exopeptidases which use a double-Glu motif to convey aminopeptidase activity. TPPII has been implicated in vital biological processes. At least one of these, antigen processing, requires the involvement of its endopeptidase activity. In order to understand the extent and molecular basis of this unusual functional promiscuity we have performed a systematic kinetic analysis of wild type *Drosophila melanogaster* TPPII and five point mutants of the double-Glu-motif (E312/E343) involving natural substrates. Unlike the known double-Glu motives of other exopeptidases, the double-Glu motif of TPPII is distinctly asymmetrical: E312 is the crucial determinant of the aminotripeptidolytic ruler mechanism. It both blocks the active-site cleft at substrate position P4 and forms a salt bridge with the N-terminus of the substrate. In contrast, E343 forms a much weaker salt bridge than E312 and it does not have a blocking role. An endopeptidase substrate can bind at relatively high affinity if the length of the substrate permits binding to several S′ sites. However, the lacking alignment of the substrate by the double-Glu motif causes the endopeptidolytic K_{cat}/K_M of TPPII to be very low.

1. Introduction

Tripeptidylpeptidase II (TPPII, EC 3.4.14.10) is an aminotripeptidase of the subtilisin type which has been implicated in several vital biological functions, such as general protein turnover, antigen trimming, control of satiety, DNA-repair, cell division, and apoptosis [1]. It constitutes the largest cytosolic protease complex in eukaryotes. The variant from *Drosophila melanogaster* forms a 6 MDa complex consisting of 40 subunits stacked into two twisted strands arranged into a spindle [2]; its structure has been determined recently [3] using a hybrid EM-X-ray approach.

Lately, evidence was presented for a structural motif of TPPII [3,4] previously found in the atomic structures of other – non-related – exopeptidases: the double-Glu motif, which is the most frequently found structural motif conferring aminopeptidase specificity to peptidases. It is present in the structures of prolyltripeptidyl peptidase (PTP, [5,6]), dipeptidyl peptidase IV (DPPIV, [7]), Tricorn F1 factor [8], and aminopeptidase N [9]. In these exopeptidases, both glutamate residues form salt bridges with the charged N-terminus of the substrate, thereby determining the position of the substrate in the active-site cleft. This binding of the N-terminus creates a molecular ruler for the precise cleavage of exopeptidase substrates after one, two, or three residues, respectively.

In addition to its aminotripeptidase activity, TPPII has been reported to possess a weak endopeptidase activity which is required for its reported function in antigen trimming (see [10] for a recent review). On the other hand, the function of TPPII as a neuropeptidase involved in cholecystokinin-8 metabolism [11], in which different peptide fragments have quite different biological functions [12], necessitates high cleavage fidelity. This precision, in turn, requires a strong discrimination against all activities other than aminotripeptidase activity. To clarify this seemingly paradoxical situation, we need to understand the role of the selectivity-mediating molecular ruler mechanism in both activities. We have shown recently that E312 and E343 are critical for exopeptidase activity of TPPII [3]. However, the binding of exo- and endopeptidase substrates to TPPII is not yet understood because in the structure of the dimer [3], only an internal loop – not a substrate or an inhibitor – is bound to the active-site cleft. The catalytic serine situated adjacent to this loop in the sequence is thus displaced from its active position, which results in an inactive form of the peptidase. TPPII dimers in solution have low activity, and full activity is attained by assembly of dimers into the spindle-shaped complex [13]. We suggested this assembly to involve a conformational rearrangement involving the loop bound to the active site [3]. Therefore, we need to study the intact TPPII complex to understand the role of the molecular ruler in exo- and endo-

Abbreviations: TPPII, tripeptidylpeptidase II; DPPIV, dipeptidylpeptidase IV; PTP, prolyltripeptidylpeptidase; Amc, 7-amido-4-methylcoumarin; SI, selectivity index; wt, wild type.

* Corresponding author. Fax: +49 89 8578 2641.
E-mail addresses: peters@biochem.mpg.de (J. Peters), schoeneg@biochem.mpg.de (A.-M. Schönegge), rockel@biochem.mpg.de (B. Rockel), baumeist@biochem.mpg.de (W. Baumeister).

0006-291X/$ - see front matter © 2011 Elsevier Inc. All rights reserved.
doi:10.1016/j.bbrc.2011.09.058

peptidase activity. To elucidate the mechanistic principle conveying aminotripeptidase selectivity to TPPII and to assess the conditions for, and significance of, the secondary endopeptidase activity, we have performed a kinetic study of the protein complex and a set of point mutants of the double-Glu motif.

2. Materials and methods

2.1. Peptide substrates

Peptides were purchased from BACHEM.

2.2. Generation of TPPII mutants

Point mutations were introduced into the *dmTPPII* gene using the QUIK-Change Mutagenesis kit (Stratagene). Cloning procedures were as described [13].

2.3. Purification of TPPII

Wild type *Drosophila* TPPII and mutants were purified from *Escherichia coli* cell lysates as described [13]. To exclude any traces of *E. coli* peptidases, purified TPPII was additionally subjected to ion exchange chromatography on HiTrap ANX and Superose 6 and the desired purity confirmed by mass spectroscopy. The integrity of the TPPII spindle complex was verified by electron microscopy of negatively stained specimen. Complex integrity in the kinetic studies was controlled by molecular sieve chromatography on Superose 6 (HR10/30).

2.4. Peptide separation

TPPII activity was routinely assayed using the fluorogenic substrate AAF-Amc [2]. To determine cleavage rates of peptides not carrying a fluorogenic reporter, acid-quenched digests were subjected to HPLC on a 150 × 4.0 mm YMC-ODS-AQ, 12 nm, S-3 mm column using a Beckman System Gold HPLC system. Peptides were eluted by 0.1% trifluoroacetic acid/0–20% acetonitrile at 0.75 ml/min and detected at 214 and 280 nm.

2.5. Determination of kinetic parameters

Digestion was carried out in Lo-Bind Eppendorf vials in the presence of 2–5 mM dithiothreitol. Peptides dissolved in 80 mM potassium phosphate, pH 7.5 were digested with wt TPPII at 0.002–0.4 mg/ml or one of its mutants at 0.02–0.2 mg/ml. Samples were incubated at 30 °C for 1 min to 24 h and digestion terminated by addition of 3 M phosphoric acid to a final concentration of 300 mM. It was ensured that the rates determined were in the linear range of the progress curve and thus corresponded to initial rates. The concentration of peptide substrates was varied in an appropriate range, depending on the respective K_M. Products were quantitated via detection at 214 nm and determination of peak areas using the molar absorption coefficients of amino acids and of the peptide bond reported in [14].

2.6. Mass spectrometry

HPLC/MS analysis of peptide digests was performed on a micro-TOF time-of-flight ESI mass spectrometer (BrukerDaltonics) coupled to an Agilent 1100 HPLC system, equipped with thermostated column compartment and autosampler (Agilent). For separations, a Varian Pursuit XRs Ultra C18 column (2.8 μm, 2.0 mm × 100 mm) was used. Samples were eluted using 0.05% TFA and a 5–80% acetonitrile gradient.

3. Results

3.1. The double-Glu motif of TPPII

To understand substrate binding to the active site of TPPII, it is necessary to know the topology of the double-Glu motif in the active enzyme as well as the sterical relationship of the two glutamates with peptides bound. Since the active site of TPPII shows homology to that of subtilisin, the known structure of the complex of subtilisin with the inhibitor Eglin C (Fig. 1A, [15]) can provide a clue of substrate alignment in the active-site cleft of TPPII. However, being an endopeptidase, subtilisin does not possess a double-Glu or related motif. To establish a tentative sterical relationship between bound substrate and the double-Glu motif of TPPII, we created a superimposition of the structures of subtilisin Carlsberg, with bound residues P42 through D46 of Eglin C, and TPPII (Fig. 1B). Since this Eglin fragment occupies binding subsites S4–S1 (Berger und Schechter nomenclature, [16]), and since, being an aminotripeptidase, TPPII only possesses the binding subsites S3–S1, we expected residue V42 (corresponding to peptide position P4) of Eglin C to be subject to a sterical clash at S4 in the superimposition. This is, indeed, the case: The S4 subsite is blocked by a ridge formed by the side chains of E312 and E343 (Fig. 1B). To obtain a clue as to how the N-terminal (P3) residue of an exopeptidase substrate might interact with the double-Glu motif in TPPII, only the residues V43 through D46 of Eglin C, corresponding to positions P3 through P1′, were considered in the superimposition. Now the carboxylate side chain of E312, which blocks the S4-position, is juxtaposed to the N-terminus of the residue in position P3, whereas the carboxylate site chain of E343 is situated laterally with respect to the substrate backbone. From this topology we predict an asymmetrical dual salt bridge of the substrate's N-terminus with the two glutamates (Fig. 1C). According to the atomic distances calculated from the superimposition, the corresponding bond lengths are 1.5 Å for E312 and 2.7 Å for E343.

We expected endopeptidase substrates of TPPII to assume a conformation similar to the bound loop residues in the crystal structure (Fig. 1D). Because P4 cannot occupy the blocked S4 position, P3 has to bend out of the cleft. Since the P3 residue of an endopeptidase substrate does not possess a free N-terminus, it cannot form a salt bridge with the carboxylate side chain of E312, but it might form a hydrogen bond with E343.

Thus, our working hypothesis for the role of the double-Glu motif in exo- and endopeptidase activity (Fig. 2) assigns a dual role to E312: this glutamate determines the three-amino-acid span of the molecular ruler by sterical limitation of the active site at S4 on one hand and by causing bound substrate to dock via a salt bridge on the other hand. Substrate docking would be expected to force the N-terminal residue to actually bind to the S3 pocket instead of assuming alternative positions at S2 or S1 (Fig. 2A). In contrast, E343 interacts with the N-terminus of exopeptidase substrates from a lateral position not posing a sterical constraint. For endopeptidase activity (Fig. 2B), we assumed that the substrate binds to the same site as an exopeptidase substrate does. In this case, residue P3 has to bend out of the active site-cleft to avoid a sterical clash of P4 with the side chain of E312. In order to test our hypothesis we performed an enzymological characterization using a mutational approach.

3.2. Mutations of the double-Glu motif

To eliminate possible salt bridges, either of the two glutamates E312 and E343 was mutated to glutamine. To remove potential sterical conflicts of endopeptidase substrates with one or both of the carboxylate side chains, either glutamate residue was

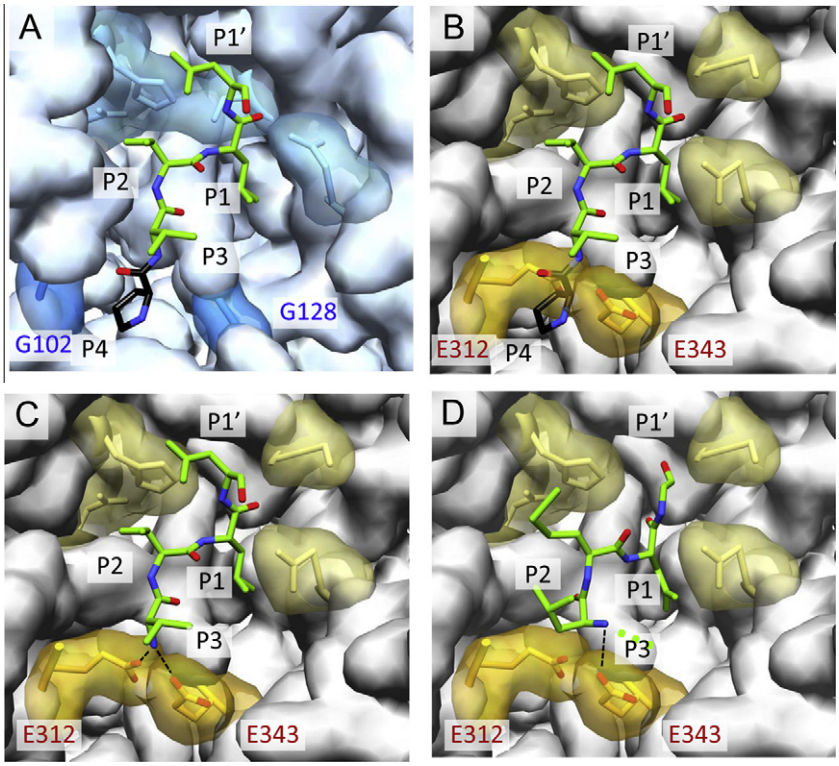

Fig. 1. Substrate binding to the double-Glu motif of TPPII. In the surface representation of the TPPII structure the residues of the catalytic triad and the Asn of the oxyanion hole are shown in light yellow, the double-Glu motif (E312/E343) is shown in intense yellow. Residues of a peptide chain bound to the active-site cleft are shown in stick representation and highlighted green. The positions are labeled according to the Berger and Schechter nomenclature [16]. (A) Binding of residues P42 through D46 of Eglin C (corresponding to P4 through P1′) to Subtilisin Carlsberg (Database ID: PDB 1CSE). (B) Superimposition of Eglin C_{42-46}, as bound to subtilisin, with the structure of TPPII (Database ID: PDB 3LXU). (C) As (B) but P42 of Eglin being deleted *in silico*. The suggested salt bridges between E312/E343 and the N-terminus of the P3 residue are indicated by dotted lines. (D) Binding of four loop residues (L457 through G460) to the active-site cleft [3]. The N-terminal continuation of the loop from L457 is indicated by green dots. A possible hydrogen bond between the E343 carboxylate and the backbone amide proton of L457/M458 is indicated by a dotted line.

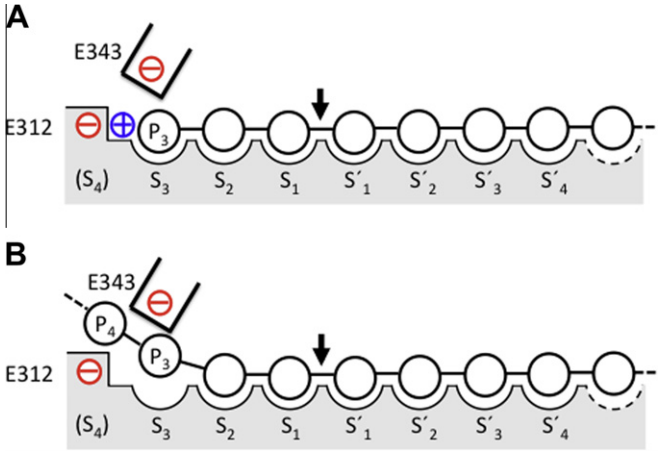

Fig. 2. Working hypothesis of exo- and endopeptidase activity of TPPII in relation to the double-Glu motif. The positions of the active-site cleft are numbered according to the Berger and Schechter nomenclature [16]. (A) Exopeptidolysis and (B) endopeptidolysis.

mutated to glycine. In addition, a double mutant E312G/E343G was created to study the effect of the complete deletion of the double Glu motif on activity. With all mutants, the structural intactness of the highly purified, spindle-shaped TPPII complex was verified by molecular sieve chromatography and by electron microscopy (Supplemental data, Fig. 1S). The TPPII complex was only slightly destabilized in all of these mutants, as judged by the occurrence of some large fragments of the complex. However, another double mutant, E312Q/E343Q, predominantly formed single strands and lower oligomers and was therefore not used in this study, since both K_M and V_{max} of TPPII depend on oligomer size [13].

3.3. Enzymological characterization of the double-Glu motif

The mutants E312Q, E312G, E343Q, E343G, and E312G/E343G were kinetically characterized using three different substrates: The standard assay substrate AAF-Amc and two natural substrates [11], the cholecystokinin fragments CCK-5 (GWMDF) and CCK-8 (DYMGWMDF). Since (amino-)exopeptidase activity requires a free N-terminus, we used these three substrates to study exopeptidase activity, whereas the endopeptidase activity of TPPII was investigated using N-terminally acylated forms of these peptides.

As endopeptidase activity we regard all peptide bond cleavages independent of the charged N-terminus. Thus, this includes cleavages after substrate positions <P3 and >P3, as well as cleavage of acylated substrate after any position. We define the exopeptidase selectivity index (SI) as the ratio of K_{cat}/K_M for the wild type, or an N-terminally free substrate, respectively, over K_{cat}/K_M for a mutant or an N-terminally acylated substrate, respectively. Acylated substrates provide selectivity indices of the whole double-Glu motif as well as information on "sterical selectivity" due to sterical clashes with either of the two glutamates. Point mutants of the double-Glu motif yield information on the contributions of individual residues to exopeptidase selectivity.

Exopeptidase activity

				AAF↓AMC	GWM↓ DF	DYM ↓GWMDF
A	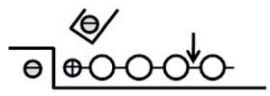	WT	V_{max}/V_{100} K_M **K_{cat}/K_M**	22 300 ± 900 435 ± 29 **1.28 x 10^5**	76 600 ± 2900 109 ± 13 **1.76 x 10^6**	12 700 ± 470 13.3 ± 1.7 **2.38 x 10^6**
B	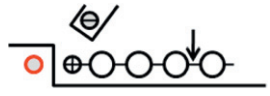	E312Q	V_{max}/V_{100} K_M **K_{cat}/K_M**	*0.06 ± 0.02* > 5000 **1.7**	*9.8 ± 2.2* > 3000 **64.8***	16.2 ± 1.2 226 ± 28.9 **262**
C	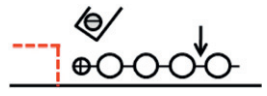	E312G	V_{max}/V_{100} K_M **K_{cat}/K_M**	*0.13 ± 0.04* > 5 000 **2.76***	4510 ± 250 1640 ± 100 **6 880**	397 ± 3 112 ± 17 **4 600**
D	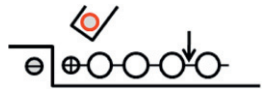	E343Q	V_{max}/V_{100} K_M **K_{cat}/K_M**	*2.6 ± 0.4* > 5 000 **65.1***	7 690 ± 2460 422 ± 189 **1.83 x 10^4**	2 600 ± 100 78.1 ± 5.0 **8.31 x 10^4**
E	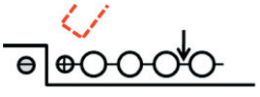	E343G	V_{max}/V_{100} K_M **K_{cat}/K_M**	4.7 ± 1.4 2 870 ± 960 **4.1**	16 700 ± 4170 566 ± 212 **6.18 x 10^4**	4 110 ± 340 96.6 ± 13.5 **1.06 x 10^5**
F	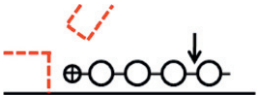	E312G/ E343G	V_{max}/V_{100} K_M **K_{cat}/K_M**	*0.005 ± 0.002* n.d. **0.15 ***	809 ± 82 618 ± 88 **3 770**	210 ± 39 229 ± 60 **2 290**

Endopeptidase activity

				Suc-AAF↓Amc	Ac-GW↓$_a$M↓$_b$D↓$_c$F	Ac-D↓$_a$YM↓$_b$GW↓$_c$MDF
G	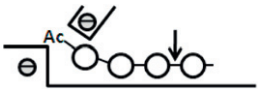	WT	V_{max}/V_{100} K_M / $K_{M\ app.}$ **K_{cat}/K_M**	*< 0.01* n.d. n.d.	(a/b) 3.7 ± 1.1 / n.d. (a/b) 1550 ± 720 / >3000 (a/b) **5.6 / 4.6**	(a/c) 3.8 ± 0.2 / n.d. 239 ± 46 / n.d. **39.5**
H	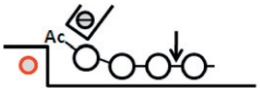	E312Q	V_{max}/V_{100} K_M **K_{cat}/K_M**	*< 0.01* n.d. n.d.	(a/b) n.d. / *0.54* (a/b) n.d / > 3000 (a/b) n.d. / **13.5**	(a/c) 5.4 ± 0.5 / n.d. 750 ± 106 / n.d. **18.0**
I	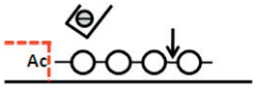	E312G	V_{max}/V_{100} K_M **K_{cat}/K_M**	*< 0.01* n.d. n.d.	(b) 668 ± 11 1490 ± 300 **1 120**	(b) 155 ± 18.0 382 ± 92 **1 010**
K	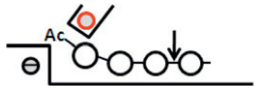	E343Q	V_{max}/V_{100} K_M **K_{cat}/K_M**	*< 0.01* n.d. n.d.	(a/b) *0.06±0.02 / 0.04±0.01* (a/b) n.d. (a/b) **1.6* / 0.9***	(a/c) *< 0.2/ <0,2* n.d. n.d.
L	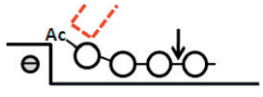	E343G	V_{max}/V_{100} K_M **K_{cat}/K_M**	*< 0.01* n.d. n.d.	(a/b) *0.03±0.01 / 0.03±0.01* (a/b) n.d. (a/b) **0.9 / 0.8***	(a/b/c) *< 0.2 / < 0.2 / < 0.2* n.d. n.d.
M		E312G/ E343G	V_{max}/V_{100} K_M **K_{cat}/K_M**	*< 0.01* n.d. n.d.	(b,c) 2 420 ± 40 / n.d. 2 110 ± 450 / n.d. **2 870** / n.d.	(b) 651 ± 30 243 ± 45 **6 700**

Fig. 3. Kinetic parameters of exo- and endopeptidase activity obtained with the wild type and mutants of TPPII. In analogy to the scheme in Fig. 2, schematic representations of the active site with bound substrate in different TPPII variants are shown on the left. Mutational changes are highlighted in red. Rates V are given in (pmol μg^{-1} min^{-1}], V at 100 μM substrate (V_{100}) is represented in italics. Note that V_{max} is defined here as specific rate and is thus proportional to K_{cat} (conversion factor: 2500). K_M (or K_M app., respectively) is given in [μM], K_{cat}/K_M is given in [s^{-1} M^{-1}]. Values were rounded to three decimals. Error margins (rounded accordingly) correspond to one S.D. K_{cat}/K_M values determined directly from initial rates at [S] < K_M are marked with an asterisk. n.d., not determined. Cleavage sites are marked a,b,c, and the corresponding kinetic parameters are marked accordingly.

3.4. Exopeptidase activity

In contrast to AAF-Amc, both natural substrates, CCK-5, and CCK-8, are cleaved efficiently by most mutants (Fig. 3), however, at more or less increased K_M and decreased V_{max}. Whereas the SI is between approx. 2×10^3 and 10^6 with AAF-Amc, it is still between approx. 25 and 3×10^4 with the natural substrates.

The impact of the mutations on the kinetic parameters is much higher for E312 (Fig. 3, rows B and C) than for E343 (Fig. 3, rows D and E). Thus, the SI values for CCK-5 and CCK-8 are approx. 25,000 and 10,000 with E312Q, but only approx. 90 and 20 with E343Q. These values imply that E312 is the crucial determinant of aminotripeptidase selectivity within the double-Glu motif, whereas E343 plays an auxiliary role. The fact that the tripeptidolytic cleavage register is maintained even in the E312G/E343G double mutant, may reflect the energetically favorable site occupation of the natural substrates CCK-5 and CCK-8. The substrate AAF-Amc is hardly cleaved by the double mutant: whereas, according to the data obtained with the E312G/E343G mutant, the SI of the double-Glu motif is approx. 1000 for CCK-8 as substrate, it is approx. 8×10^5 for AAF-Amc (Fig. 3, row A vs. F). It follows that binding pockets S1–S3 alone do not provide enough affinity for a TPPII substrate to be bound and aligned for cleavage.

The high exopeptidase selectivity of the mutations is in agreement with the observation that cleavages of CCK-5 and CCK-8 by wt TPPII deviating from the canonical tripeptide register were not detectable, implying a cleavage fidelity >approx. 99.9%.

3.5. Endopeptidase activity

Endopeptidolytic cleavage by TPPII may occur in two ways: If cleaved after sequence position >2, acetylated substrates would be expected to be subject to a sterical clash with E312 (see Fig. 2B). Alternatively, the cleavage may occur at sequence position <3, thus avoiding a clash. Both patterns are observed in the cleavage of CCK-5 and CCK-8.

The endopeptidase activity of the wild type and the mutants E312Q, E343Q, and E343G, all of which possess a side chain on residue 312, is very low, with SI > 10^5. In contrast, the endopeptidase activity of mutants lacking the E312 side chain, E312G (Fig. 3, row I) and E312G/E343G (Fig. 3, row M) is comparable to the activity on the corresponding exopeptidase substrates. In these two mutants, the exopeptidolytic cleavage register is maintained. Thus, the acetyl group is obviously accommodated without a clash at position S4, which implies that – as hypothesized – the side chain of E312 blocks the S4 position of the active site cleft.

In contrast to the deletion of the side chain of E312, the deletion of the side chain of E343, as in E343G (Fig. 3, row L), does not lead to an increase of endopeptidase activity. Therefore, the E343 side chain does not appear to contribute to the sterical constraints imposed by the molecular ruler. Neither does it promote endopeptidase activity, since K_{cat}/K_M of Ac-GWM↓DF is not increased by the presence of the side chain of E343.

Whereas AAF-Amc binds to the S1 through S3 site, although at very low affinity, binding of Suc-AAF-Amc is not detectable at all. In contrast, Ac-CCK-8, which binds only to the S1, but also to the S′ sites, has a K_M of approx. 240 μM with wild type TPPII (Fig. 3, row G), which reflects the requirement of the S′ sites for the binding of endopeptidase substrates.

3.6. Exo- vs. endopeptidase activity

In exopeptidase activity, and much more so in endopeptidase activity, the contribution of the V_{max} decrease to the lowering of K_{cat}/K_M exceeds that of the K_M increase. Thus, it is not primarily the affinity of the substrate for the active site that determines the selectivity, but rather the alignment of the substrate by the double-Glu motif, which in turn determines the cleavage rate. This is particularly apparent from the extremely low cleavage rates of acylated substrates, which lack the alignment by both salt bridges.

A quantitative comparison of exo- and endopeptidase activity for a certain substrate requires the cleavage register to be the same for both cleavage modes. The partial cleavage of CCK-5 in the register Ac-GWM↓DF permits such a comparison. For GWM↓DF vs. Ac-GWM↓DF the SI of wild type TPPII is approx. 380,000. This value reflects the effects of both the lack of the salt bridge and the sterical clash at E312. For the E312Q mutant the "sterical" SI for GWM↓DF vs. Ac-GWM↓DF is only approx. 5. It follows that the discrimination against endopeptidase activity is mainly attributable to the failure of the substrate to form a salt bridge with E312 whereas the sterical clash of the substrate at E312 plays a minor role.

To exclude that the effect on activity exerted by the salt bridges between the double-Glu motif and the N-terminus of the substrate is attributable to structural perturbations of TPPII, we deleted the charge on the substrate as opposed to deleting it on the enzyme. The endopeptidase substrate used for this purpose was Ac-WMDF, which differs from GWMDF only in the lack of the N-terminal amino group and which is cleaved in the fashion Ac-WM↓DF. We observed a decrease of $V_{100\mu M}$ of approximately 10^7-fold upon deletion of the N-terminal charge, which is attributable to the lack of both salt bridges between enzyme and substrate.

4. Discussion

The kinetic data for exo- and endopeptidolytic cleavage presented above confirm the hypothesis that E312 is both the blocking site determining the length of the molecular ruler and the principal docking site binding the charged N-terminus of the substrate. In contrast, E343 has an auxiliary function in coordinating exopeptidase substrates, but there is no evidence of a role in endopeptidase activity.

The agreement of our data with the prediction confirms that the topology of the double-Glu motif in the crystal structure of inactive dimers matches the situation in the assembled, active complex.

Particular care had to be devoted to exclusion of structural perturbations as causes for the effects of the mutations on the kinetic data. In general, the structure of the TPPII complex is very sensitive even towards single point mutations [3], and in turn, the kinetic parameters of TPPII depend on the integrity of the complex [13]. The partial dissociation and/or aggregation of two double-Glu mutants E305Q and E331Q of murine TPPII [4] as well as the low stability of the E312Q/E343Q double mutant of *Drosophila* TPPII, which was not used in this study, reflect the delicate embedment of the double-Glu residues of TPPII in the overall structural context.

The pronounced length asymmetry of charge bridges formed by the double-Glu motif in TPPII stands in contrast to the situation in PTP and DPPIV, where the salt bridges determined from the respective X-ray structure [5,7] are similar to each other in length and significantly longer than predicted for TPPII. In accordance with the shorter salt bridges, TPPII shows a much higher exopeptidase selectivity than PTP (calculated from [6]), and DPPIV (calculated from [17]), as revealed by a comparison of the SI values for double-Glu mutations of the three peptidases (Table 1A). Selectivity data obtained with N-terminally blocked substrate and wild type enzyme is available for aminopeptidase N [18]. Again, TPPII has a much higher selectivity (Table 1B).

An aspect masked out in studies using assay substrates carrying a fluorophore in position P1′ is the contribution of the S′-sites to the catalytic efficiency. We show here that in TPPII, substrate binding to these sites may significantly increase K_{cat}/K_M. This in turn results in lower selectivity for longer peptides, because the

Table 1
Comparison of exopeptidase selectivity indices. The SI was determined (A) with wt vs. double-Glu mutants and (B) with non-acylated vs. acylated substrates. NA, naphtylamine; Ts, toluene sulfonate; aminopep. N, aminopeptidase N. The numbers for DPPIV and PTP were calculated from K_{cat}/K_M values given in the respective references.

Peptidase (substrate)	Mutation	K_{eff} (WT)/K_{eff}(Mut.)
A		
DPPIV (GP-Ts, Ref. [17])	E205K	52
	E206L	
PTP (GAP-ßNA, Ref. [6])	E205A	n.d.
	E636A	120
TPPII (AAF-Amc)	E312Q	75,300
	E343Q	1970
B		
Peptidase	Substrate	$K_{eff}(NH_2\text{-pep})/K_{eff}$(acyl-pep)
Aminopep. N (Ref. [18])	(NH_2/Suc)-AAF-Amc	185
TPPII	(NH_2/Suc)-AAF-Amc	$>10^7$
	CCK-5/Ac-CCK-5	382,000

extremely poor binding of endopeptidase substrates to the S1 through S3 sites is partially compensated by binding to the S′ sites. However, the strong salt bridge formed by E312 still provides a very high exopeptidase selectivity with CCK-5 and CCK-8 (Table 1B). In fact, the paramount importance of this salt bridge for the catalytic efficiency suggests that the very strong discrimination against endopeptidase activity is a general property of TPPII.

A remarkable aspect of our mutational analysis – probably reflecting TPPII's evolutionary descent from subtilisin – is the observation that only the removal of the side chain of E312 turns TPPII into an endopeptidase with K_{cat}/K_M of the order of $10^3\ M^{-1}\ sec^{-1}$ with CCK-5 and CCK-8, rendering the endopeptidolytic efficiency similar to the exopeptidolytic efficiency of E312. This drastic change can be effected by a single base exchange in the nucleotide sequence. A point mutation affecting assembly and abolishing activity was previously discovered with human TPPII [19]. It should be considered, that endopeptidase activity found with TPPII *in vivo* might result from a mutation such as E312G.

Acknowledgments

We wish to thank the Core Facility of the MPI of Biochemistry, Martinsried for cell cultivation, and mass spectrometry and Marietta Peters for technical assistance. This work was supported by funding of the Deutsche Forschungsgemeinschaft (Ro-2036/5-11 and SFB 594).

Appendix A. Supplementary data

Supplementary data associated with this article can be found, in the online version, at doi:10.1016/j.bbrc.2011.09.058.

References

[1] B. Tomkinson, A.C. Lindas, Tripeptidyl-peptidase II: a multi-purpose peptidase, Int. J. Biochem. Cell Biol. 37 (2005) 1933–1937.
[2] B. Rockel, J. Peters, B. Kühlmorgen, R.M. Glaeser, W. Baumeister, A giant protease with a twist: the TPPII complex from *Drosophila* studied by electron microscopy, EMBO J. 21 (2002) 5979–5984.
[3] C.K. Chuang, B. Rockel, G. Seyit, P.J. Walian, A.M. Schonegge, J. Peters, P.H. Zwart, W. Baumeister, B.K. Jap, Hybrid molecular structure of the giant protease tripeptidyl peptidase II, Nat. Struct. Mol. Biol. 17 (2010) 990–996.
[4] A.C. Lindas, S. Eriksson, E. Jozsa, B. Tomkinson, Investigation of a role for Glu-331 and Glu-305 in substrate binding of tripeptidyl-peptidase II, Biochim. Biophys. Acta 1784 (2008) 1899–1907.
[5] K. Ito, Y. Nakajima, Y. Xu, N. Yamada, Y. Onohara, T. Ito, F. Matsubara, T. Kabashima, K. Nakayama, T. Yoshimoto, Crystal structure and mechanism of tripeptidyl activity of prolyl tripeptidyl aminopeptidase from *Porphyromonas gingivalis*, J. Mol. Biol. 362 (2006) 228–240.
[6] Y. Xu, Y. Nakajima, K. Ito, H. Zheng, H. Oyama, U. Heiser, T. Hoffmann, U.T. Gartner, H.U. Demuth, T. Yoshimoto, Novel inhibitor for prolyl tripeptidyl aminopeptidase from Porphyromonas gingivalis and details of substrate-recognition mechanism, J. Mol. Biol. 375 (2008) 708–719.
[7] M. Engel, T. Hoffmann, L. Wagner, M. Wermann, U. Heiser, R. Kiefersauer, R. Huber, W. Bode, H.U. Demuth, H. Brandstetter, The crystal structure of dipeptidyl peptidase IV (CD26) reveals its functional regulation and enzymatic mechanism, Proc. Natl. Acad. Sci. USA 100 (2003) 5063–5068.
[8] P. Goettig, H. Brandstetter, M. Groll, W. Gohring, P.V. Konarev, D.I. Svergun, R. Huber, J.S. Kim, X-ray snapshots of peptide processing in mutants of tricorn-interacting factor F1 from *Thermoplasma acidophilum*, J. Biol. Chem. 280 (2005) 33387–33396.
[9] K. Ito, Y. Nakajima, Y. Onohara, M. Takeo, K. Nakashima, F. Matsubara, T. Ito, T. Yoshimoto, Crystal structure of aminopeptidase N (proteobacteria alanyl aminopeptidase) from *Escherichia coli* and conformational change of methionine 260 involved in substrate recognition, J. Biol. Chem. 281 (2006) 33664–33676.
[10] G. Preta, R. de Klark, R. Gavioli, R. Glas, The enigma of tripeptidyl-peptidase II: dual roles in housekeeping and stress, J. Oncol. 2010 (2010).
[11] C. Rose, F. Vargas, P. Facchinetti, P. Bourgeat, R.B. Bambal, P.B. Bishop, S.M. Chan, A.N. Moore, C.R. Ganellin, J.C. Schwartz, Characterization and inhibition of a cholecystokinin-inactivating serine peptidase, Nature 380 (1996) 403–409.
[12] J. Bradwejn, Neurobiological investigations into the role of cholecystokinin in panic disorder, J. Psychiatry Neurosci. 18 (1993) 178–188.
[13] G. Seyit, B. Rockel, W. Baumeister, J. Peters, Size matters for the tripeptidylpeptidase II complex from *Drosophila*: the 6-MDa spindle form stabilizes the activated state, J. Biol. Chem. 281 (2006) 25723–25733.
[14] B.J. Kuipers, H. Gruppen, Prediction of molar extinction coefficients of proteins and peptides using UV absorption of the constituent amino acids at 214 nm to enable quantitative reverse phase high-performance liquid chromatography-mass spectrometry analysis, J. Agric. Food Chem. 55 (2007) 5445–5451.
[15] W. Bode, E. Papamokos, D. Musil, The high-resolution X-ray crystal structure of the complex formed between subtilisin Carlsberg and eglin c, an elastase inhibitor from the leech *Hirudo medicinalis*. Structural analysis, subtilisin structure and interface geometry, Eur. J. Biochem. 166 (1987) 673–692.
[16] A. Berger, I. Schechter, Mapping the active site of papain with the aid of peptide substrates and inhibitors, Philos. T Roy. Soc. B 257 (1970) 249–264.
[17] C.A. Abbott, G.W. McCaughan, M.D. Gorrell, Two highly conserved glutamic acid residues in the predicted beta propeller domain of dipeptidyl peptidase IV are required for its enzyme activity, FEBS Lett. 458 (1999) 278–284.
[18] D. Chandu, A. Kumar, D. Nandi, PepN, the major Suc-LLVY-AMC-hydrolyzing enzyme in *Escherichia coli*, displays functional similarity with downstream processing enzymes in archaea and eukarya – implications in cytosolic protein degradation, J. Biol. Chem. 278 (2003) 5548–5556.
[19] B. Tomkinson, B.N. Laoi, K. Wellington, The insert within the catalytic domain of tripeptidyl-peptidase II is important for the formation of the active complex, Eur. J. Biochem. 269 (2002) 1438–1443.